A triple deck model of ripple formation and evolution

P.-Y. Lagrée[a)]
Laboratoire de Modélisation en Mécanique, U.M.R. CNRS 7607, Université Pierre et Marie Curie, Boîte 162, 4 place Jussieu, 75005 Paris, France

(Received 27 August 2002; accepted 10 May 2003; published 2 July 2003)

The two-dimensional laminar quasisteady asymptotically simplified flow with mass transport of sediments is solved over an erodible bed in various laminar hydraulic regimes (infinite depth, finite depth subcritical or supercritical, nondisturbed boundary layer). Compared to the boundary layer thickness, the bump is supposed longer and thinner and the triple deck theory is used. Furthermore, the flow is linearized. Next, a simplified mass transport equation is obtained which includes the two following phenomena: there is a flux of erosion when the skin friction goes over a threshold value, and concentration of sediment in suspension is convected but falls at a constant settling velocity. It is shown that two ingredients (convection of the longitudinal flux or particles and advanced response of the skin friction to the bump changes) are necessary to produce (except in the supercritical regime which, in this flux convected model, is always stable) a band of amplified spatial frequencies. Furthermore, putting the effect of slope limitation makes long wave stable (in the infinite depth case). Examples of evolution in various regimes are presented, wave trains of ripples are created and merge in a unique bump. A very long time is required for this process. This coarsening appends except in the infinite depth case when the effect of slope limitation is turned on: in this case a train of several bumps fills the computation domain. © *2003 American Institute of Physics.*
[DOI: 10.1063/1.1588305]

I. INTRODUCTION

Let us consider the deformation of a bump immersed in a flow. This bump is made of an erodible material which may be convected and diffused in the flow. Practical cases would consist in dune of sand in water of various depth, or dune of sand in air. This kind of flow is of course very important for environmental problems and a vast literature refers to these problems since Exner in 1925 (Yang,[1] Bagnold, Fredsøe and Deigaard,[2] Nielsen,[3] Sauerman and Herrmann,[4] Sauerman, Kroy, and Herrmann[5]). This problem is very complex because all mechanical effects are linked (the flow depends on the shape of the bump which depends on the flow which erodes or deposits sediments on the soil modifying again the flow).

These erosion/sedimentation problems have been solved by various techniques with various approaches. Even recent studies use simplified physical models to compute the flow Andersen,[6] Nishimori *et al.*;[7] most of which use continuum models of mechanics; the flow is now computed with direct solution of Navier–Stokes equations with turbulent models Andersen *et al.*,[8] Andersen and Fredsøe,[9] Kroy, Sauerman, and Herrmann,[4] and Sauerman, Kroy, and Herrmann.[5] But, ultimately, all these studies have to look at the flow near the soil. This is the boundary layer itself (which is not so well solved by NS k-ϵ solvers). That is why they finally turn to a simplified law issued from asymptotic analysis by Jackson and Hunt,[10] where the final important ingredient is the velocity near the wall coming from the turbulent boundary layer theory: the logarithmic profile law. Previous studies often solved the problem by integral boundary layer theory (Plapp,[11] Akiyama and Stefan[12] or Zeng and Lowe[13]).

These boundary layer approaches are pertinent because all the phenomena take place near the wall, where the velocity changes abruptly on a small scale: the boundary layer thickness. Here we use the framework of the triple deck theory (Neiland,[14] Smith,[15] and for recent developments Sychev *et al.*,[16] Smith,[17] Bhattacharyya *et al.*[18]) which allows a strong coupling between the laminar boundary layer and the ideal fluid. The flow separation is not a problem: even more, the triple deck was created to compute the separation of the boundary layer. As conditions for this description the flow is supposed to be two-dimensional (for sake of simplicity), quasisteady (erosion and sedimentation are a slow process) and it is assumed laminar. This last hypothesis is maybe the stronger one, but we will see that we recover some results obtained by Charru *et al.*[19] and Fowler.[20] In the first one, a laminar theory has been proposed in the case of a Couette flow, and we will see that taking this theory in the long wave case leads to a triple deck case; in the second one, Fowler[20] recovers the same equation too, but starting from other hypothesis (in fact the turbulent flow is modelled by a laminar one of viscosity equal to a mean turbulent viscosity). The concentration of sediments in the flow is supposed small enough to unaffect viscosity and density of the flow: we do not use models of re suspension as in Schlafinger *et al.*[21] The concentration of sediment is a continuous function. A less simplified model using interacting boundary layer theory in subcritical flow has been presented in Lagrée.[22] In fact, triple deck is a true asymptotic limit of Navier–Stokes equations as

[a)]Electronic mail: pyl@ccr.jussieu.fr

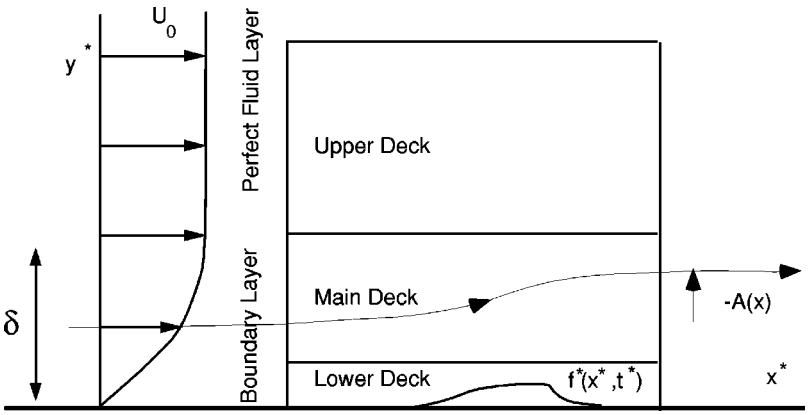

FIG. 1. A rough sketch of the flow: a boundary layer of thickness δ encounters a very small hump so that only the linear sheared part of the profile is perturbed. In fact an interacting structure is created, this perturbation on a small longitudinal scale near the wall (lower deck) perturbs the boundary layer core (main deck) so much that the ideal fluid layer (upper deck) is linearly perturbed as well, retroacting onto the lower deck.

Re number tends to infinity, and it leads to simple linearized results linking the skin friction distribution on the dune to its shape. That is why this simplified point of view will here be employed (Neiland[14] and Smith[15]).

As our aim is to present a oversimplified model, we will use the terms ''dune'' or ''ripples'' in an improper way because we deal only with very simplified models far from reality. From our model equation a structure will emerge from variation of an initially flat wall, and this structure will be called train of ''dunes'' or ''ripples.'' We may say, in the subcritical case, that this objects are dunes. When using the Hilbert integral, this structure may be called ripples if we consider a flow of infinite depth of water, but ripples or dunes if we consider an air flow (there is no scale in our equations). First we shall present the classical triple deck equations in the various regimes (Sec. II A), and next a simplified concentration evolution (Sec. II B). Thus we link the flow to the movement of the erodible bed. The numerical method is shortly explained in Sec. III. The linear temporal stability of the system is presented (Sec. IV A 1) validating the numerical solution. Simulations of several initial bumps are presented (Secs. IV A 1–IV B 1). Finally (Sec. IV B 2) we shall discuss the long time evolution resulting in a coarsening in a unique dune (except in the slope effect case in an infinite depth regime).

II. THE COUPLED MODEL

A. Dynamical aspect: The triple deck

1. The triple deck

In Fig. 1 we present a rough sketch of the flow and the decks. There is a flow of incoming water over a flat bottom under a quiet atmosphere. In the limit of laminar two-dimensional (2D) steady flow at high Reynolds number, the water has an basic thickness h_0. If this depth of liquid goes to infinity the problem is independent of the existence of the free surface. The basic flow splits into two layers: the ideal fluid layer of thickness h_0 where the velocity is of constant value U_0 (U_0 free stream velocity) and the boundary layer, the Froude number is $\mathrm{Fr}=U_0^2/(gh_0)$. Let us call L the developing length of the boundary layer, $L\,\mathrm{Re}^{-1/2}$ is then the thickness of the viscous layer (see Schlichting[23]). Of course $h_0 \gg (L\,\mathrm{Re}^{-1/2})$, which means that the boundary layer has not yet merged in a single layer of fluid [see Higuera[24,25] for the study of the self-induced jump when $h_0=(L\,\mathrm{Re}^{-1/2})$ and Lagrée[26] for its thermal counterpart], in fact the present theory is included in Higuera's one for small values of x^* (variables with stars are with dimensions).

Notice that the incoming velocity profile is here selected to be a Blasius one [defined by the function U_B, such as the longitudinal velocity in the boundary layer is $u^*(x^*,y^*)=U_0U_B(\tilde{y}\bar{x}^{-1/2})$ where $\bar{x}=x^*/L$ is the longitudinal abscissa and $\tilde{y}=y^*/(L\,\mathrm{Re}^{-1/2})$ the boundary layer thickness]. In fact any given boundary layer profile is relevant, scales have then to be rewritten using its thickness. An extension of this theory should be constructed so that is included a slip effect which may arise when the bottom is porous.

We next introduce in the flow a small bump of relative thickness ε (compared to the boundary layer thickness $L\,\mathrm{Re}^{-1/2}$) at the position $x^*=L$ (or $\bar{x}=1$). In this layer of thickness $\varepsilon L\,\mathrm{Re}^{-1/2}$ the velocity is linear in $\tilde{y}$, so u^* is scaled by εU_0, pressure/convective balance suggests that the pressure is scaled by $\varepsilon^2\rho U_0^2$. On purpose that the problem presents the maximum number of terms (least possible degeneracy, Van Dyke[27]), including pressure, convective terms and a viscous term, x^* is scaled by $x^*=L+\varepsilon^3 Lx$. Time should then be scaled by $\varepsilon^3 L/(\varepsilon U_0)$, but if we call T the scale of the erosion/sedimentation [$t^*=Tt$, cf. the equation of evolution of the bottom in the next section, Eq. (21)], we will have $\varepsilon^2 L/U_0/T \ll 1$, and t is only a parameter associated to the bump shape.

With these usual triple deck scales (Neiland,[14] Stewartson and Williams,[28] Smith,[15] Sychev *et al.*,[16] Gajjar and Smith,[29] Bowles and Smith[30]), the problem in the ''lower deck'' is simply

$$\frac{\partial}{\partial x}u+\frac{\partial}{\partial y}v=0, \tag{1}$$

$$u\frac{\partial}{\partial x}u+v\frac{\partial}{\partial y}u=-\frac{d}{dx}p+\frac{\partial^2}{\partial y^2}u. \tag{2}$$

It means that near the wall there exist scales such that a non linear problem (with convection, diffusion and pressure gradient) has to be solved. Boundary conditions are no slip condition on the bottom

$$u(x,y=f(x))=0, \quad v(x,y=f(x))=0, \tag{3}$$

and the asymptotic matching between the ''lower deck'' and the ''main deck.'' This latter is in fact the boundary layer itself: ''far'' from the wall with the focused scales we are ''near'' the wall in the boundary layer scales (the transverse variable is here $\tilde{y}$, with $\varepsilon y=\tilde{y}$, and the longitudinal dimensionless velocity is here $\tilde{u}$ of scale U_0). The perturbation of the boundary layer at the scale $\varepsilon^3 L$, at position $\bar{x}=1$, gives the function $(-A)$ which represents the deflection of the streamlines:

$$\tilde{u}=U_B(\tilde{y})+\varepsilon A U_B'(\tilde{y})+\cdots,$$

$$\tilde{v}=-\frac{A'(x)U_B(\tilde{y})}{\varepsilon^2(\mathrm{Re}^{1/2})}+\cdots, \quad -\frac{\partial}{\partial\tilde{y}}\tilde{p}=0+\cdots.$$

The matching between the top of the lower deck ($y\to\infty$) and the bottom of the main deck ($\tilde{y}\to 0$) yields

$$\lim_{y\to\infty}(\varepsilon u(x,y))=\lim_{\tilde{y}\to 0}\tilde{u}(x,\tilde{y}),$$

i.e.,

$$\lim_{y\to\infty}u(x,y)=U_B'(0)(y+A). \tag{4}$$

The latter means that the incoming velocity is linear, this means that upstream we recover the boundary layer profile:

$$u(x\to-\infty,y)=U_B'(0)y, \quad v(x\to-\infty,y)=0. \tag{5}$$

Finally, the deflection of the stream lines induced in the lower deck (function $-A$) is transmitted by the main deck, perturbating the ''upper deck'' (which is the third layer involved). This perturbation is a kind of suction velocity $-\varepsilon^{-2}(\mathrm{Re}^{-1/2})(dA/dx)$, or a perturbation of the displacement thickness by an amount of $\varepsilon(L\,\mathrm{Re}^{-1/2})(-A)$. In the layer of ideal fluid, the pressure responds to this boundary layer displacement by the pressure modification. This fixes the value of the scale: $\varepsilon=(L/h_0)\mathrm{Re}^{-1/2}$. The final coupling relation between p and A is

$$p=\frac{-A}{\mathrm{Fr}-1}. \tag{6}$$

In the subcritical regime p and $-A$ have the opposite sign ($\mathrm{Fr}<1$), and a decrease of the water level ($-A<0$) is produced at the perturbation (Baines[31]); the opposite is true in the supercritical regime [$\mathrm{Fr}>1$, then p and $(-A)$ have the same sign] (see Gajjar and Smith[29] or Kluwick *et al.*[32] for details on the upstream influence).

If h_0 is very high in comparison to the bump length and L, the free surface is at infinity. The gauge is $\varepsilon=\mathrm{Re}^{-1/8}$ and we may ultimately recover the Hilbert case

$$p=-\frac{1}{\pi}\int\frac{-A'}{x-\xi}d\xi. \tag{7}$$

This is the classical incompressible result. Another result is obtained when the perturbation of the bump on the boundary layer (main deck) is so small that no displacement occurs, which reads

$$A=0. \tag{8}$$

This case corresponds to several different configurations: it corresponds to a bump of length equal or smaller to the size of the boundary layer itself $\varepsilon^3=\mathrm{Re}^{-1/2}$, but this result is the one found by Plantier[33] for a Couette flow. This is in fact the configuration found in Charru *et al.*:[19] they identify this regime as the ''deep viscous regime.'' Finally, in the half Poiseuille case (corresponding to a fully developed laminar flow), this case is the Smith[34] result, which is used by Fowler.[20]

Interesting enough, the Hilbert case degenerates in the case ($A=0$: no perturbation in the boundary layer) when the bump becomes shorter and shorter (Smith *et al.*[35]). So having a given water depth, depending on the size of the perturbations one can meet either a subcritical case, either an Hilbert case or a nondisturbing case. In the numerical applications we will focus on these last two cases.

2. Dynamical system for the fluid

The final dependence in $U_B'(0)$ and $\mathrm{Fr}-1$ can then be removed by a straightforward rescaling [which is deduced from the fact that Eqs. (1), (2), and (5) are invariant for any Y when $x\to Y^3x$, $y\to Yy$, $u\to Yu$, $p\to Y^2p$, and $A\to YA$]. So the interacting problem is

$$\frac{\partial}{\partial x}u+\frac{\partial}{\partial y}v=0, \tag{9}$$

$$u\frac{\partial}{\partial x}u+v\frac{\partial}{\partial y}u=-\frac{d}{dx}p+\frac{\partial^2}{\partial y^2}u, \tag{10}$$

$$u(x,y=f(x))=0, \quad v(x,y=f(x))=0, \tag{11}$$

$$\lim_{y\to\infty}u(x,y)=y+A. \tag{12}$$

With either

(i) the infinite depth case

$$p=-\frac{1}{\pi}\int_{-\infty}^{\infty}\frac{-A'}{x-\xi}d\xi,$$

with

$$x=(x^*/L-1)U_B'(0)^{5/4}/(\mathrm{Re}^{-3/8}),$$

$$y=(y^*/L)U_B'(0)^{3/4}/(\mathrm{Re}^{-5/8}),$$

$$p=(p^*/(\rho U_0^2))U_B'(0)^{-1/2}/(\mathrm{Re}^{-2/8}),\ \text{etc.}$$

(ii) The no displacement case $A=0$, which either is the limit of the preceding one when the length of the bump is the boundary layer thickness, either exists in half Poiseuille flow or either exists in Couette flow.

(iii) The subcritical case $p=A$ and the supercritical $p=-A$, both with

$$x=(x^*/L-1)U_B'(0)^5|\mathrm{Fr}-1|^3/(\mathrm{Re}^{-3/8}),$$

$$y=(y^*/L)U_B'(0)^2|\mathrm{Fr}-1|^{-1}/(\mathrm{Re}^{-5/8}),$$

$$p=(p^*/(\rho U_0^2))U_B'(0)^2|\mathrm{Fr}-1|^{-2}/(\mathrm{Re}^{-2/8}),\ \text{etc.}$$

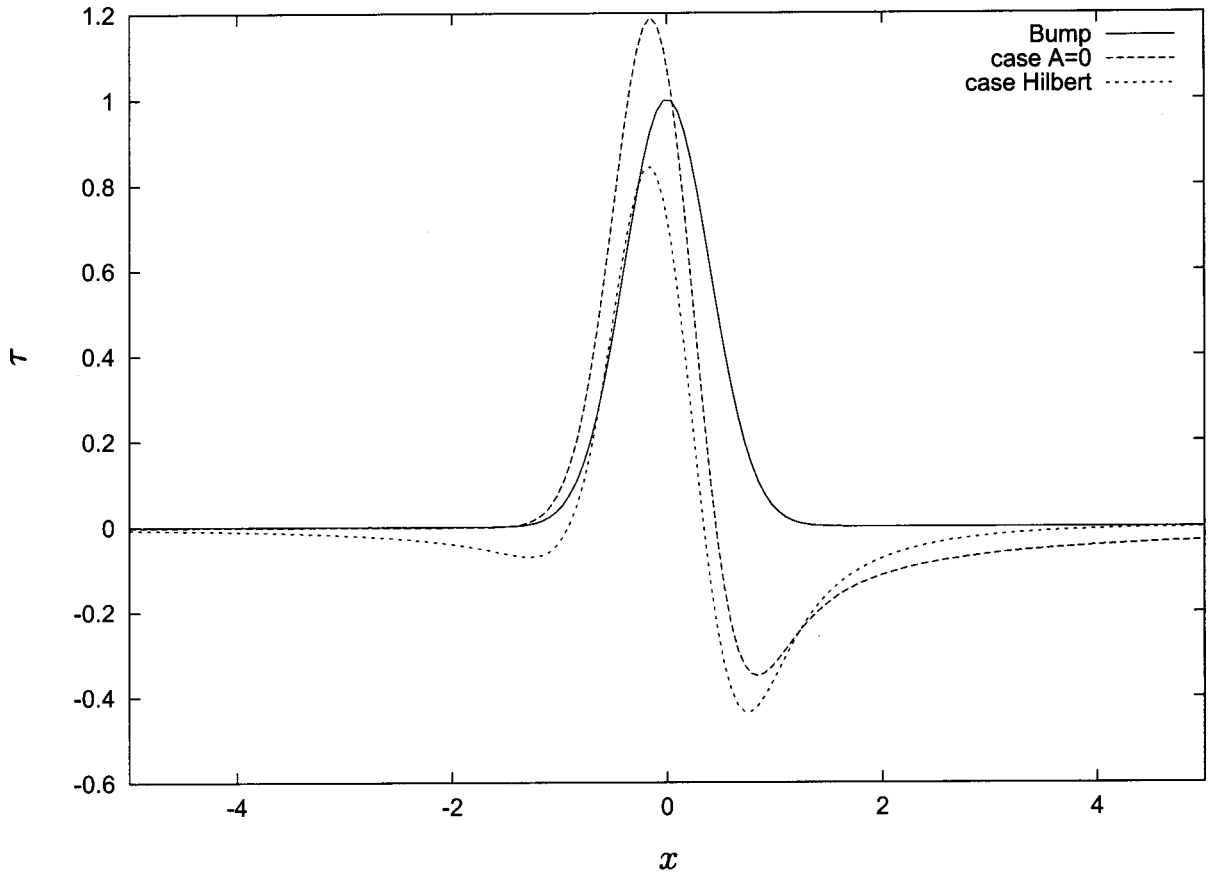

FIG. 2. The linear solution (in the triple deck scales) for the perturbation of the wall shear function of x, in the $A=0$ case, and in the Hilbert case $p=-\pi^{-1}\int(x-\xi)^{-1}(-A')d\xi$. The bump perturbation is here $e^{-\pi x^2}$. The case $A=0$ leads to no upstream influence, the Hilbert case leads to a small upstream influence: the skin friction anticipates the bump. The skin friction is extreme before the maximum of the bump. Skin friction is larger in the wind side than in the lee side.

3. Final linearization: Law between the topography and the skin friction

The unperturbed solution of (9) and (10) is simply $u=y$, $v=0$, $p=0$. It implies that, at the small longitudinal scale, the boundary layer thickness does not evolve and the velocity profile remains linear near the wall. The linearized solution of (9) and (10) around this shear profile in Fourier space is straightforward and leads to $\beta^* FT[p]=FT[(A+f)]$ where $\beta^*=(3\,\mathrm{Ai}'(0))^{-1}(-ik)^{1/3}$.

The linearized solution of the ideal fluid problem ("upper deck") may be written $\beta_{pf}FT[p]=FT[(A)]$ with $\beta_{pf}=1/|k|,0,1,-1$ [respectively, (6) for (7) and (8), Fr<1 and Fr>1], so

$$FT[p]=\frac{FT[f]}{\beta^*-\beta_{pf}}. \tag{13}$$

The linearized perturbation of the skin friction (τ) is then (Ai is the Airy function)

$$FT[\tau]=\frac{(-ik)^{2/3}}{\mathrm{Ai}'(0)}\mathrm{Ai}(0)FT[p]. \tag{14}$$

This well-known relations (13) and (14) gives the final response of the fluid: it links the topography change to the shear stress. It will be very useful in the sequel as the shear stress is believed to control the flux of sediments.

In Fig. 13 in the Appendix we present a numerical solution of the problem [in a zero displacement case (8) of Smith[34]] in order to discuss the influence of the nonlinearity of the solution and the boundary layer separation. We see in the Appendix, that even for bump leading to flow separation, the prediction of formula (14) is correct, the main advantage of this triple deck model being that flow separation is effectively constructed without the approximations of Kroy, Sauerman, and Herrmann[4] or Andreotti *et al.*[36]

In Figs. 2 and 3 we draw the solution of the perturbation of the skin friction for the various cases. When Fr<1 in (6) or in the infinite depth case (7) or in the "Couette" (8) case, we see that the skin friction is always extreme before the maximum of the bump (the wind side of the bump). In the subcritical case and in the "Couette case," there is no influence of the downstream part of the flow to the upstream. Case (7) gives a small upstream influence; on the opposite the supercritical case [(6) with Fr>1] leads to a strong upstream influence: perturbation exists before the bump. In this sole case the wall shear stress is not extreme before the maximum of the bump; in the three other ones the skin friction is "in advance" with the bump shape.

Knowing the response of the fluid to any perturbation (in the selected framework) we now examine the transport equation.

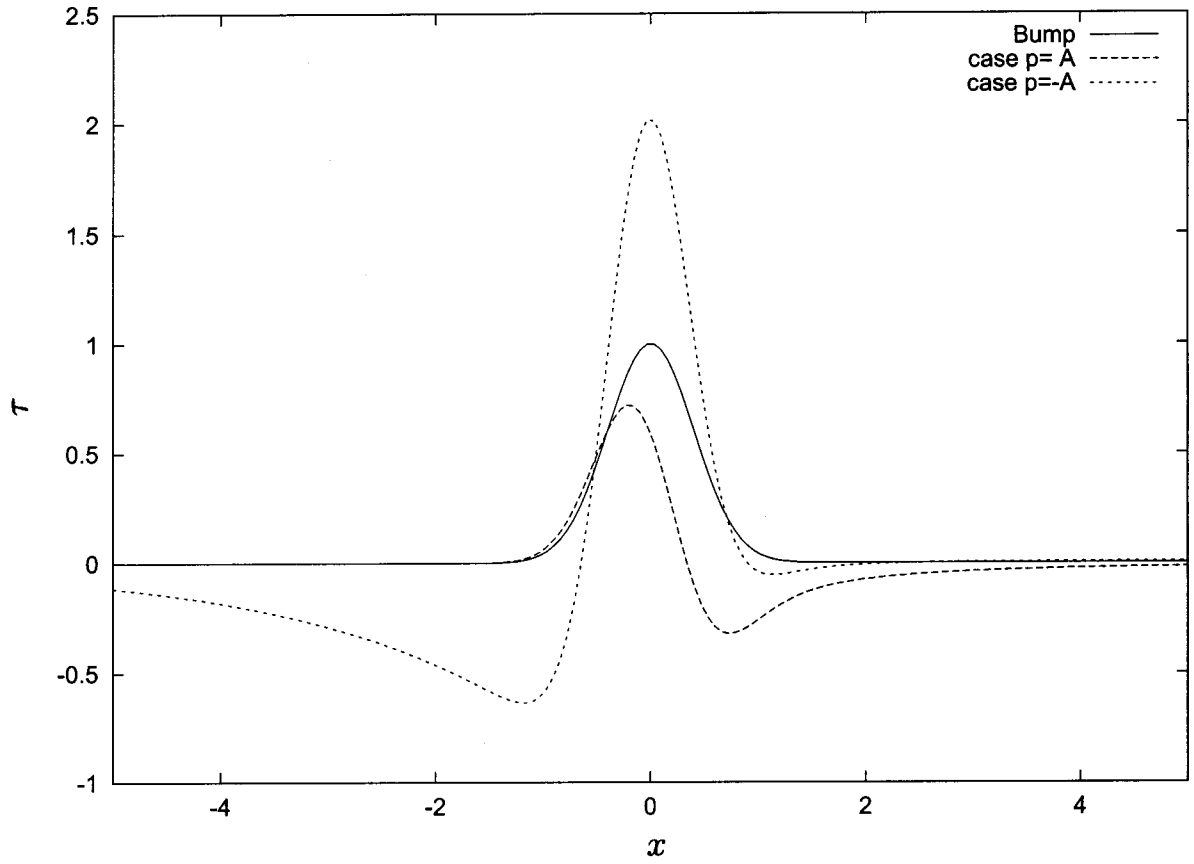

FIG. 3. The linear solution (in the triple deck scales) for the perturbation of the wall shear function of x, in the $p=-A$ case, and in the $p=A$. The bump perturbation is here $e^{-\pi x^2}$. The case $p=A$ (subcritical) leads to no upstream influence, the case $p=-A$ (supercritical) leads to a strong upstream influence: the skin friction anticipates the bump. The skin friction is extreme before the maximum of the bump only in the fluvial case

B. Transport equation

1. The equation

Together with the dynamical equations of the flow one has to solve the quasistatic mass conservation of the particles in the laminar flow (Fig. 4). We aim to derive a simple law linking the flux of sediments to the skin friction. Of course real transport of sand takes place in the turbulent regime, but here to be coherent with our simplification we write sediment transported in the laminar case. The concentration is supposed small enough so that it does not interact with the fluid motion. We suppose a simple Fick law and we define S the Schmidt number (ratio of viscosity by diffusion). We assume that there is a settling constant velocity (written $-V_f^*<0$). This means that we suppose that the equation of momentum conservation for the sediments is solved so that the speed of the sediments is u, $v-V_f^*$. With those restrictive hypothesis the dimensionalized transport equation of suspended sediments is

$$u^*\frac{\partial}{\partial x^*}c^*+(v^*-V_f^*)\frac{\partial}{\partial y^*}c^*=\frac{\nu}{S}\left(\frac{\partial^2}{\partial x^{*2}}c^*+\frac{\partial^2}{\partial y^{*2}}c^*\right). \tag{15}$$

In the literature (Noh and Fernando,[37] Fredsøe,[2] Izumi and Parker,[39] Nielsen,[3] Fredsøe and Deigaard,[2] Seminara[38]) it is written in the turbulent regime. The integral counterpart of this equation may be taken in integrating form $y^*=0$ to h_0. A characteristic thickness of suspended sediment under the settling and diffusive effects is $(\nu/(SV_f^*))$, see Fredsøe and

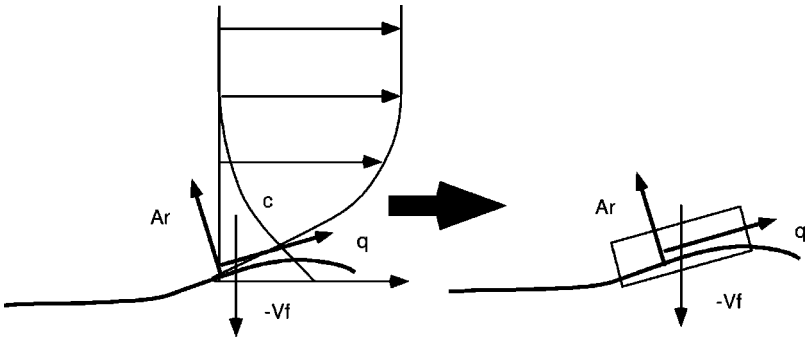

FIG. 4. The concentration of sediments c (decreasing with altitude) is passively transported in the flow, it is submitted to diffusion and to a constant falling velocity $-V_f^*<0$. The skin friction puts sediments in suspension (source term A_r), those two contributions change the total flux of convected sediments q (left figure). A simplified view is displayed on the right part where a simple mass balance is done (in a small control volume): the sediment flux q is changed by loss proportional to q (due to sedimentation) and by gain proportional to A_r the pick up function.

Deigaard,[2] here we suppose that $h_0 \gg \nu/(SV_f^*)$. We suppose as well that the settling velocity is of order $(\delta/L)U_0$, where U_0 is the characteristic longitudinal velocity and L the longitudinal scale. As a consequence, boundary layer arguments allow to neglect the longitudinal second order derivative in (15). We define, as Anderen and Fredsøe,[9] the flux with dimensions: $q^* = \int u^* c^* \, dy^*$, this is the flux of convected sediments. So, transverse integration of (15) yields

$$\frac{\partial}{\partial x^*} q^* + (V_f^*) c^*_{\text{bottom}} = -\frac{\nu}{S}\left(\frac{\partial}{\partial y} c^*\right)_{\text{bottom}}. \tag{16}$$

In fact this equation is valid for a turbulent flow too, as far as the right-hand side (RHS) is the total flux at the wall. We define A_r^* the flux as

$$A_r^* = -\frac{\nu}{S}\frac{\partial c^*}{\partial y^*}\bigg|_0. \tag{17}$$

The boundary conditions of (15) are clear upstream and on the top: here we suppose no incoming sediment flux on the incoming flow and no sediments are poured. The problem stems from the bottom. We have to link the transverse flux $[A_r^*$, the RHS of (15)] to the skin friction. The boundary condition for the suspended concentration is taken as follows:

$$A_r^* = \beta\left(H\left(\frac{\partial u^*}{\partial y^*}\bigg|_0 - \tau_s^*\right)\right)\left(\frac{\partial u^*}{\partial y^*}\bigg|_0 - \tau_s^*\right)^{\gamma}, \tag{18}$$

where $H(x)$ is the Heaviside function $[H(x<0)=0,\ H(x>0)=1]$, β is of order one and γ (common values are 1, 3/2 or 3, we will take $\gamma=1$ in practice). Formulas (17) and (18) mean that there is a threshold value of the skin friction $(\partial u^*/\partial y^*)|_0$: if it is larger than this threshold value τ_s^*, then the flow erodes the bump; otherwise erosion occurs $((\partial c^*/\partial y^*)|_0 = 0)$.

The latter of (18) is common (written with the Shields parameter) in the literature of erosion/sedimentation (Van Rijn formula, or Pieter-Meyer formula cf. Nielsen[3]), but other formulas may be found (Yang[1]). Notice that it is mostly written in a turbulent regime so that the friction velocity is used instead of the skin friction.

An effect of slope may be introduced as well [leading to a multiplicative coefficient like $[1-\lambda(\partial f^*/\partial x^*)]$ (Komarova and Hulscher[40]) or changing the threshold, τ_s^* in $[\tau_s^* + \lambda(\partial f^*/\partial x^*)]$]. The latter expression will be used in the next paragraph, when we will discuss its influence on stability. Notice that here we have changed a bit the classical law: in the literature, the bed load is taken to be equal to the proceeding formula,

$$q^* = B^* A_r^*, \tag{19}$$

where B^* is an *ad hoc* coefficient, see Yang,[1] but here we suppose that it is the transverse flux (17) that is equal to (18). Note that final laws linking the flux q^* and the excess of skin friction are finally always like (19) (even Charru and Mouilleron-Arnould, who take a Schlafinger description, reobtain this formula in the linearized case). We will see in the next paragraph that (16) may be rewritten (25) as $\partial q^*/\partial x^*$ plus a term proportional to q^* equals to A_r^* of (18).

Finally, the net flux of particles at the wall has two contributions: erosion $[(\nu/S)(\partial c^*/\partial y^*)|_0]$ and sedimentation $(V_f^* c^*|_0)$; this total flux deforms the bed (of shape f^*, n is porosity) according to

$$(1-n)\frac{\partial f^*}{\partial t^*} = V_f^* c^*|_0 + \frac{\nu}{S}\frac{\partial c^*}{\partial y^*}\bigg|_0. \tag{20}$$

According to (16), q^* may be reintroduced, and this equation is written as

$$(1-n)\frac{\partial f^*}{\partial t^*} = -\frac{\partial q^*}{\partial x^*}, \tag{21}$$

which is common in the literature (Exner law: Izumi and Parker,[39] Nielsen,[3] Fredsøe and Deigaard[2]).

It is of course at this point that the time scale T associated with the preceding equation is chosen: the deformation is done at a very long scale compared to the hydrodynamic scale (so the flow is quasisteady).

2. The final simplification in a shear flow

We rewrite (15) with triple deck scale, in the linearized case $(u=y)$, the velocity profile is linear (V_f is suitably rescaled):

$$y\frac{\partial}{\partial x} c - V_f \frac{\partial}{\partial y} c = S^{-1}\frac{\partial^2}{\partial y^2} c \tag{22}$$

integrating (22) over the lower deck yields

$$\frac{\partial}{\partial x}\int_0^\infty (yc)\,dy - (-V_f c_0) = -S^{-1}\left(\frac{\partial c}{\partial y}\right)_0. \tag{23}$$

The subscript 0 denotes the wall. From the conditions at $y=\infty$, and if we define as in the preceding paragraph the dimensionless "bed load" as $q = \int_0^\infty (yc)\,dy$ (i.e., the flux of sediment in a thin layer near the wall), the first term is the derivative of q. The second one can be rewritten with q, if we guess that c_0 is likely to be proportional to q. We may justify roughly this strong hypothesis as follows: we observe that as $-V_f c_0 \simeq (\partial c/\partial y)_0$, the solution for the concentration behaves more or less as $c_0 \exp(-\kappa y S V_f)$, with κ of order one. In fact as we suppose that this parameter remains nearly constant, we are allowed to write that

$$q \simeq c_0 (SV_f)^{-2}\int (\eta \exp(-\kappa\eta)\, d\eta) \tag{24}$$

which means that q is proportional to c_0 the value of the concentration at the wall. Consequently (23) may be approximated by

$$\frac{\partial}{\partial x} q + Vq = \beta\left(H\left(\tau - \tau_s - \lambda\frac{\partial f}{\partial x}\right)\left(\tau - \tau_s - \lambda\frac{\partial f}{\partial x}\right)\right)^{\gamma}, \tag{25}$$

where V is a new constant linked to S, V_f and the other physical parameters, and supposed to be here of order

one (H is the Heaviside function), τ being the perturbation of the skin friction induced by the topography f which evolves as

$$\frac{\partial f}{\partial t} = -\frac{\partial}{\partial x} q. \tag{26}$$

As suggested before, this last equation, which is dimensionless, gives the time scale of the phenomena: the flow is quasistatic compared to the slow topography evolution. As displayed in a simplified way in Fig. 4, (25) is a simple mass balance: the sediment flux q is changed by loss proportional to q (due to sedimentation) and by gain proportional to A_r the pick up function.

3. Notes

Notice that Eq. (25) contains a derivative term that we may reinterpret as an effect of inertia: for example, if the skin friction goes under the threshold value, the flux q is not instantaneously put to zero but relaxes smoothly in the streamwise direction. Furthermore, we present here only a linear relation for q, the nonlinearity is in the threshold. We may compare this to Sauerman *et al.*[5] While they obtain a saturated flux q_s function of an excess of skin friction, our notations would result in something like: $q_s = (\beta/V)(H(\tau - \tau_s)(\tau - \tau_s)^{\gamma}$. They obtain with their model that the total flux relaxes on q_s as $l_s(\partial/\partial x)\, q = q(1 - q/q_s)$. Thus, linearizing as $q = q_s + \overline{q}$, the equation for the excess of flux is $l_s(\partial/\partial x)\overline{q} + \overline{q} = 0$ (they take the length scale as function of the excess of flux, this is the constant $1/V$ of our model). Re-adding the two contributions, we see that Eq. (25) is not so far from their analysis, if linearized.

Theories linked to BCRE descriptions (Bouchaud *et al.* [41]) will add another term with which the left-hand side of (25) will read

$$\alpha \frac{\partial}{\partial t} q + \frac{\partial}{\partial x} q + Vq, \tag{27}$$

this unsteady term (as in Valance and Rioual[42]) is not relevant in our analysis because of the quasisteady nature of the flow.

To be noticed here too, is the fact that the slope effect is very crude: it is a kind of ''viscous'' diffusive dissipation ($\partial_t f \propto \partial_x^2 f$). Hence, it presents a very strong drawback as it makes flat any topography (by diffusion). A better way would be introducing a slope limitation mechanism for the topography which would remove this drawback. For example, Boutreux *et al.*[43] propose a simple model of avalanche without any diffusive term.

III. NUMERICAL SOLUTION OF THE FINAL PROBLEM

We have to solve at each time step t: first, a steady linearized triple deck problem, which for the given dune shape $f(x,t)$, gives the distribution of τ [the perturbed skin friction (13) and (14)]; second, the mass transport equation (25) which gives q; third, the shape of the bump is modified according to (26) for the next time step.

The solution is achieved in Fourier space for (13) and (14), but with a return in physical space for (25). This return in the physical space deals with the unique ''nonlinearity'' of the problem which is the Heaviside function taken in (25), the ''pick up'' relation. The update of the bump shape is done using an Adams Bashford two steps in time method.

At initial time $t = 0$, we impulsively introduce a bump of given equation $f(x, t = 0)$ (which may be a random sum of cos with a very small amplitude). We choose a typical set of order one parameters for the models: $\beta = O(1)$, $\tau_s = O(1)$, $\lambda = O(0.1)$, and $V = O(1)$, the domain is defined by its half length L_x which we will vary: $-L_x < x < L_x$.

The occurrence of the term $\partial_x q$ is very favourable for the stability of the numerical scheme as it allows values of Δt to be of the same order than $\Delta x = 2L_x/(N-1)$ (N number of points for the Fourier transform). If this term is not present, then as (25) is explicit in $\partial_x f$, then Δt must be smaller that $V\Delta x^2/(\lambda\beta)$. The number N has to be large enough to obtain accurate results, a too crude computation does not lead to the final coarsening, in practice $\Delta t \simeq 0.05$, $N \geqslant 512$, so that $\Delta x \leqslant 0.125$.

IV. RESULTS

A. Initial time: Linear results and temporal stability of an initial flat topography

1. Dispersion relation

If τ_s is negative, a steady uniform solution of system [(13) and (14)–(25) and (26)] is $\tau = 0$, $f = 0$ and $q = (\beta/V)(-\tau_s)^{\gamma}$. The linear stability analysis around this basic flow is then straightforward [and is fully valid as long as $H(\tau - \tau_s) = 1$]; looking for modes in $e^{\sigma t - ikx}$ and here taking $\gamma = 1$ we simply find that

$$\sigma = \left(\frac{ik\beta}{V - ik}\right)\left(\frac{(-ik)^{2/3}}{\mathrm{Ai}'(0)}\mathrm{Ai}(0)\frac{1}{\beta^* - \beta_{pf}} + ik\lambda\right), \tag{28}$$

with $\beta^* = (3\,\mathrm{Ai}'(0))^{-1}(-ik)^{1/3}$, $\beta_{pf} = 1/|k|, 0, 1, -1$ [respectively, for (7) and (8), Fr<1 and Fr>1]. The parameter β will often be taken equal to V thereafter.

2. Linear stability analysis

First we examine the most simple case with no slope effect, $\lambda = 0$, and with no effect of inertia on q (with $V = \beta \gg 1$, i.e., $q = \tau$), then all the spatial frequencies are unstable for the subcritical, infinite depth, and the $A = 0$ called ''deep viscous regime'' by Charru *et al.* The supercritical case is stable for $k < 2.4$.

Introducing λ (with $V = \beta \gg 1$, i.e., $q = \tau - \lambda\partial_x f$) leads to a cutoff frequency k_m (depending on the parameters). The high frequencies (which behave as $-\lambda k^2$) are stable for all models; for $k > k_m$ we have $\mathrm{Re}(\sigma) < 0$. For small frequencies ($0 < k < k_m$) the configuration remains unstable (except in the Fr>1 case where values of λ larger than 0.0947 fully stabilize the problem).

Now, if we introduce the $\partial_x q$ term [$V = \beta$, $\lambda = 0$, i.e., $(1/V)\partial_x q + q = \tau$], it has a stabilizing effect (as λ) for large k and a band of amplified frequencies (the small frequencies, $0 < k < k_m$) exists in all the cases except for the supercritical one which is always stable.

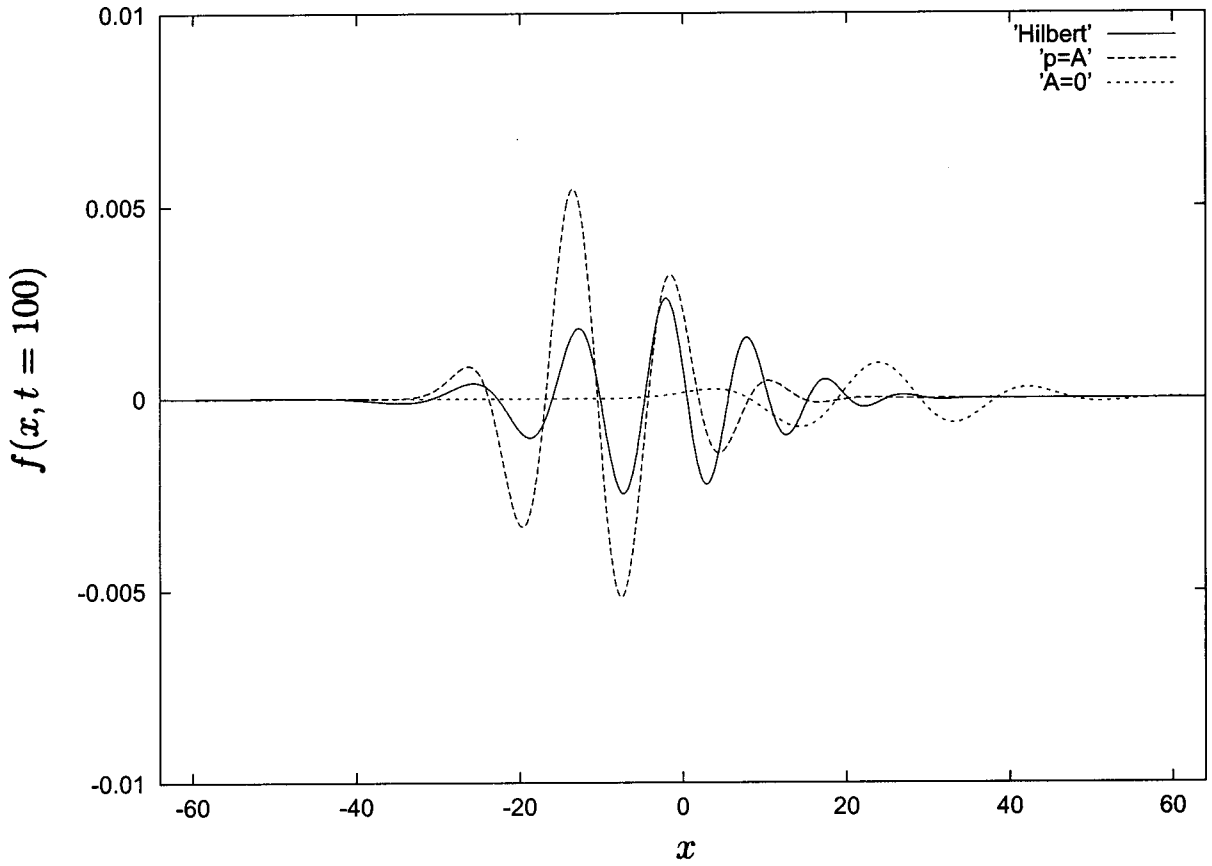

FIG. 5. The topography at time $t=100$ for the three unstable regimes ($\beta=V=\gamma=1$, $\lambda=0$, $L_x=64$ $\tau_s=-0.1$). At time $t=0$, a random noise of level 0.001 was introduced. The spatial frequency k_M giving the larger $\mathrm{Re}(\sigma)$ in the band $0<k_M<k_m$ has been selected.

To illustrate this instability, we start from a random small topography and wait for a sufficient long time (but being here always in the linear regime): we observe numerically that the value of the wave number which maximizes σ of (28) (say k_M) is effectively the value leading to a maximum for the energy spectrum ($k_M=0.59$ if $\beta_{pf}=1/|k|$, $k_M=0.49$ if $\beta_{pf}=1$ and $k_M=0.31$ if $\beta_{pf}=0$). This is shown in Fig. 5 where the wall shape is plotted at time $t=100$. The case with no displacement is wider than the others (it has the smaller k_M), it is faster as well [it has the largest phase velocity $\mathrm{Im}(\sigma(k_M))/k_M$] and it has the smallest height [it has the smallest amplification factor $\mathrm{Re}(\sigma(k_M))$].

3. Note on the lag

Notice here that the idea of Kennedy[44] (or Engelund and Fredsøe[45]) is reobtained in a certain sense. They introduced an advance between the velocity (here skin friction) and the the topography (with the law $q=\tau$) due to the fact that the boundary layer was unknown. Suppose that the response of the skin friction is a simple change of phase $\exp(-i\phi)$, with $-\pi/2<\phi<\pi/2$, the skin friction is in advance (the maximum is before the maximum of the bump); if $\phi>0$, the skin friction is "late" if $\phi<0$. The amplification rate (if $q=\tau$) is $\sigma=ik\exp(-i\phi)$, which gives temporal amplification for all frequencies if the skin friction is in advance ($\phi>0$).

Now if we introduce $\partial_x q$, the left-hand side $(1/V)\partial_x q+q$ may be reinterpreted as the Taylor's series of $q(x+1/V)$. Hence $1/V$ is a kind of lag: q and the velocity are not in phase, q is late. The same has been obtained by Sauerman *et al.*[5] (but with a nonlinear term added, and the possibility of saturation of q which is not put here). This allows to write (remember that here $V=\beta$) the amplification rate $\sigma=[ikV/(V-ik)]\exp(-i\phi)$, which gives $\mathrm{Re}(\sigma)>0$, temporal amplification, for $0<k<V\tan(\phi)$. The slope effect has the same interpretation: $-\lambda\partial_x f$ may be interpreted as a term of a Taylor's series. Those two effects work in the same reverse direction: they are "late" compared to the topography.

The conclusion for our proposed models is first, that the skin friction must be in advance with the topography to have instabilities and second that if there is no introduction of a lag $1/V$ or λ one cannot introduce a wavelength selection, the topography is temporally unstable for any spatial frequency.

4. Focusing on slope effect in Hilbert case

The Hilbert, $A=0$ and $\mathrm{Fr}<1$ cases are unstable for small wave number [in the $(\partial_x q)/V+q=\tau$ case]. We nevertheless focus here on the Hilbert case in which we introduce the slope effect ($-\lambda\partial_x f$). As already mentioned, the first effect of the slope stabilizes large wave numbers in any case. But, the other limit of small wave numbers is changed for the infinite depth case: as observed previously with no slope effect, large wavelength ($k\to 0^+$) are always amplified. Those wavelengths may be damped if the slope effect is introduced. Near $k=0$, σ of (28) expands as

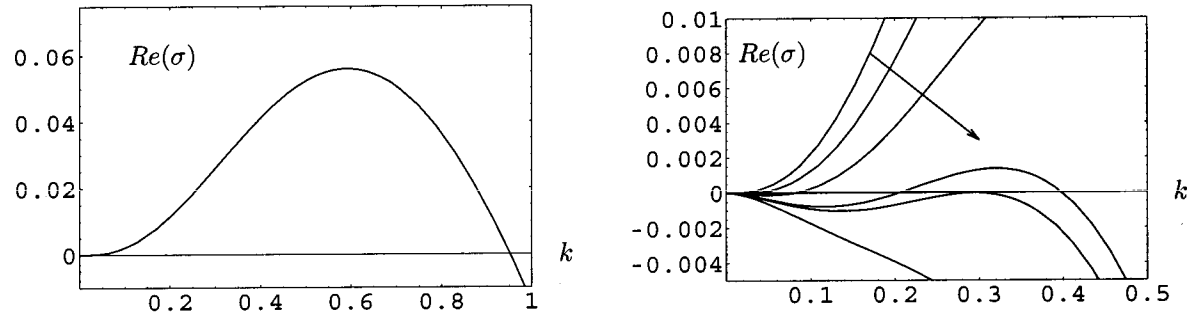

FIG. 6. Infinite depth case (Hilbert case). The real part of σ for $\beta=V=\gamma=1$ as function of the wavelength k. In the left figure $\lambda=0$, there is no slope effect. In the right figure, we focus on the small k which are amplified when $\lambda=0$, but are damped for $\lambda>0$ (following the arrow, from up to down $\lambda=0$, $\lambda=0.1$, $\lambda=0.2$, $\lambda=0.3$, $\lambda=0.316$, and $\lambda=0.4$).

$$\sigma=-\left(\frac{\beta\lambda k^2}{V}\right)-\frac{(-1)^{1/6}\beta\,\mathrm{Ai}(0)k^{8/3}}{V\,\mathrm{Ai}'(0)}-\frac{i\beta\lambda k^3}{V^2}+O(k)^{10/3}. \tag{29}$$

The k^3 term disappears if $q=\tau-\lambda\partial_x f$. The effect of the slope (λ) in the Hilbert case allows always the damping of the long wavelengths. There is then a band of amplified k which excludes the value $k=0$ (see Fig. 6).

The $A=0$ and $\mathrm{Fr}<1$ cases turn out to be different. In those configuration, the small wave numbers are always amplified.

We guess that if $\sigma>0^+$ for $k>0^+$, the large wavelength will be amplified, and as occurs a bound due to the numerical solution (the size of the box), a single bump may be present in the domain. This result will be seen numerically in the paragraph dealing with long time behavior.

Here we have in fact observed that the small k behavior is dependent on the exact solution of the flow through the exact development at the origin. Only the infinite depth case allows a wave selection. For example, if, as in the preceding section, we put a simple change of phase between the

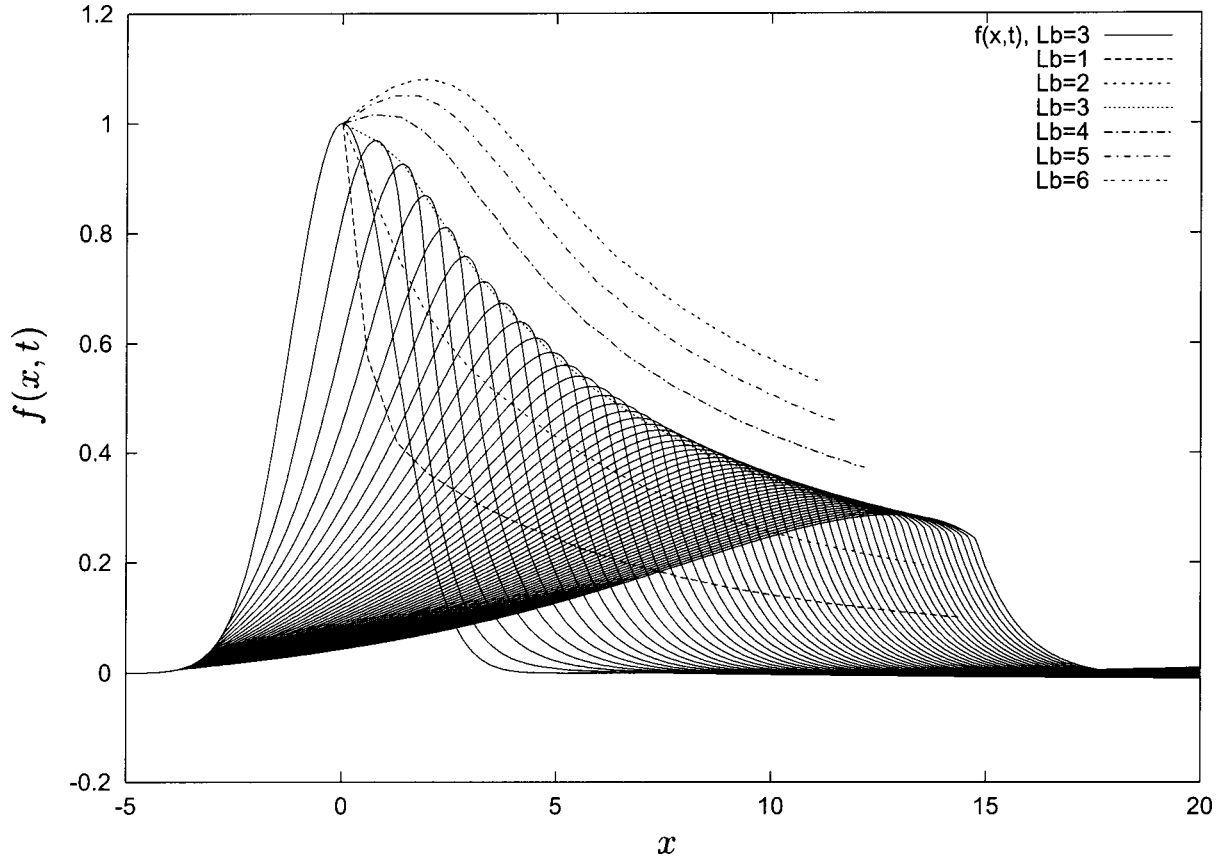

FIG. 7. Influence of the initial width L_b of a bump $\exp(-\pi(x/L_b)^2)$, the maximum of the bump is plotted for $L_b=1$, 2, 3, 4, and 5 for $t<100$; $f(x,t)$ is plotted as well (for $t=0,2,4,6,\ldots,100$ with $L_b=3$). The larger the bump, the smaller its velocity; $\beta=1$, $\gamma=1$, $V=1$, $\lambda=0$, and $\tau_s=0$.

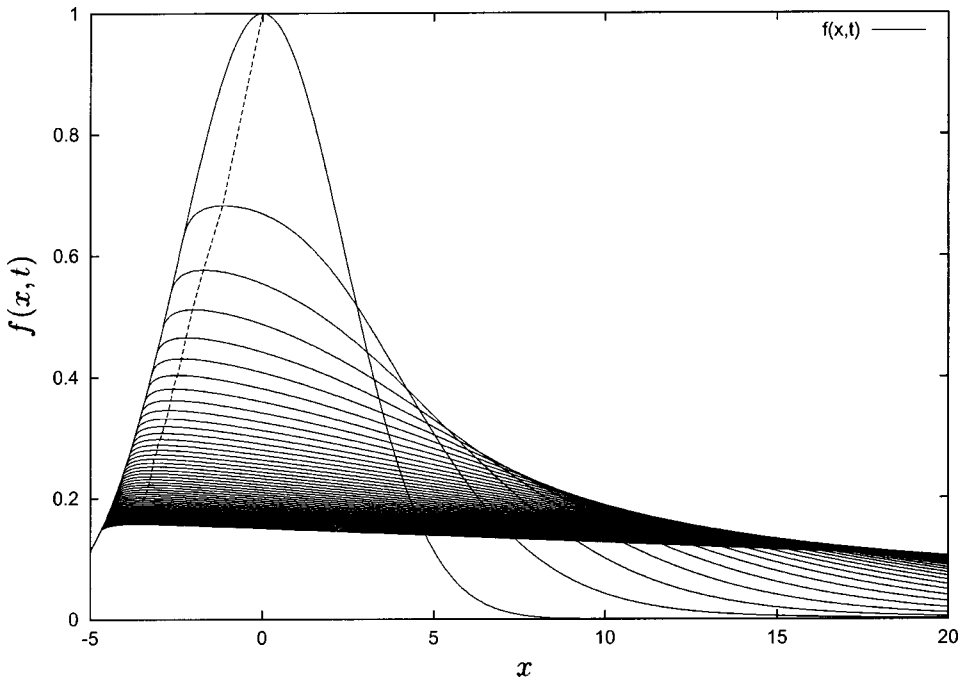

FIG. 8. Destruction of a bump $\exp(-\pi(x/6)^2)$ in the supercritical régime, with $\beta=1$, $\gamma=1$, $V=1$, $\lambda=0$, and $\tau_s=0$; the maximum of the bump is plotted for $t<100$, it is moving upstream; $f(x,t)$ is plotted as well (for $t=0,2,4,6,\ldots,100$).

topography and the skin friction ($\exp(-i\phi)$) we do not reobtain this slope effect. This same phenomena of wave selection is observed in Blondeau analysis[46] in an oscillating flow and in Richard's one[47] in a turbulent case. This is named ''ripple mode.'' Our analysis is in fact too far from Richardson's one to use his definitions (roughly speeking roughness controls the ripples, and depth controls the dunes). As the turbulence plays as a complicating factor (introducing the roughness scale), the occurrence of the Hilbert solution is hidden.

B. Time evolution of the system

1. Moderate time: Examples of qualitative influence of the different parameters

Before looking at long time behavior, in this section we allow some parameters to vary in order to observe qualitatively some various phenomena.

First we observe on one example (Hilbert case) the influence of the bump length on the movement of the bump. Starting from a bump of Gaussian shape, $\exp(-\pi(x/L_b)^2)$ we

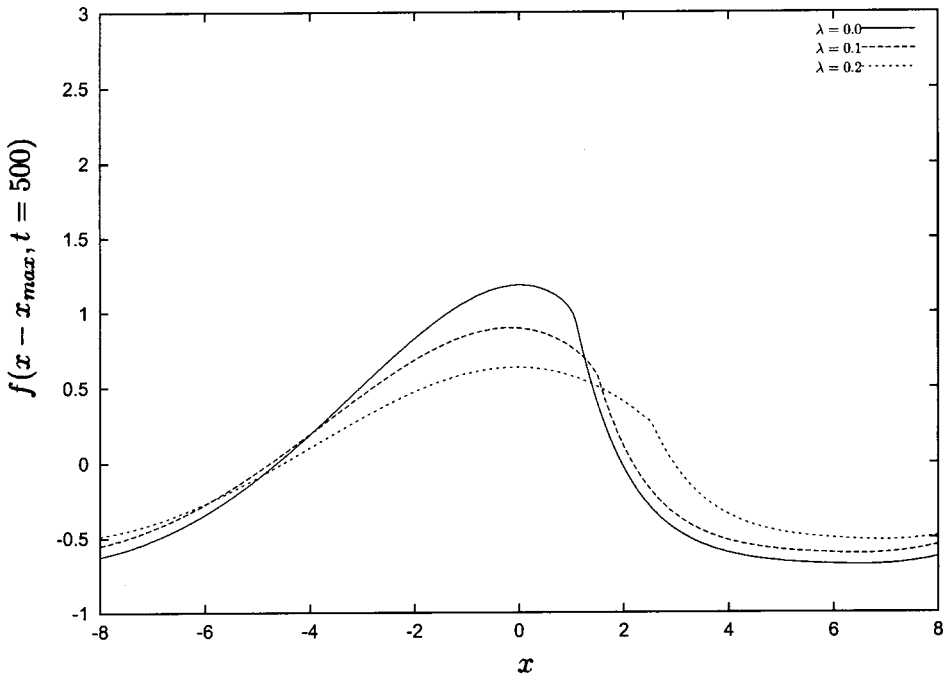

FIG. 9. Bump shape at time $t=500$, at an intermediate time at which four bumps coexist with $\beta=1$, $\gamma=1$, $V=1$, $\tau_s=-0.05$, Hilbert case. The slope effect is observed on the curves $\lambda=0$, $\lambda=0.1$, and $\lambda=0.2$ (the curves are shifted to place the maximum at the origin), notice the kink effect which arises even at $\lambda=0$ [it corresponds to the point where the RHS of (25), A_r, is zero].

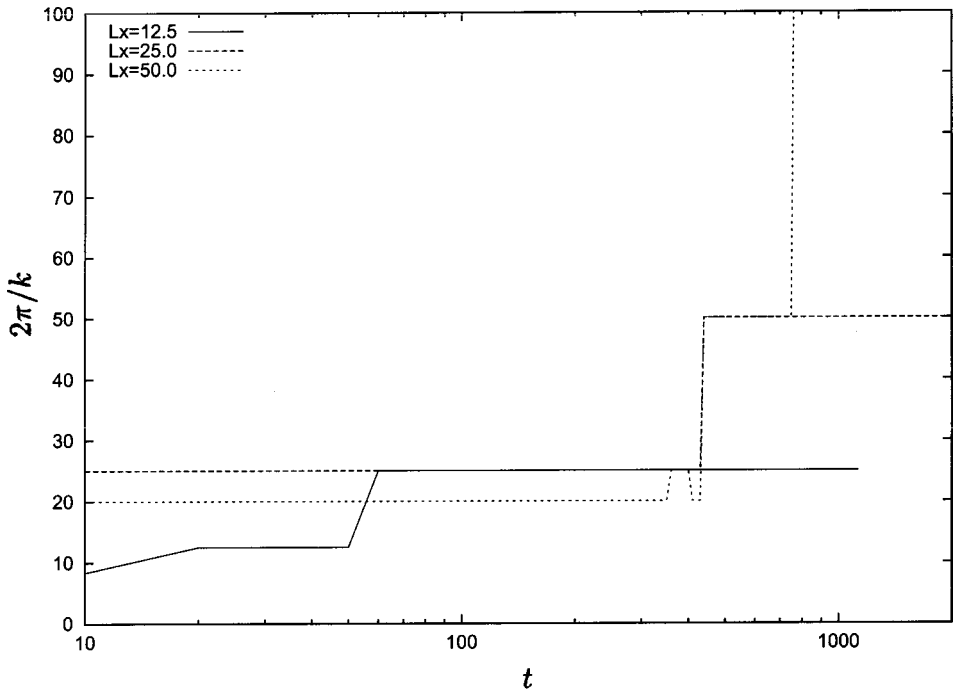

FIG. 10. The wavelength $2\pi/k$ of the maximum of the bump spectrum versus time, corresponding mostly to the number of bumps present in the domain, is plotted as function of time (log scale), here in the case $A=0$. As time increases, there is less and less bumps present in the domain, finally a single bump fills it $2\pi/k_{\text{final}}=2L_x$. Here, $L_x=12.5$, 25, and 50. The long waves are unstable in such a way that the final length of the bump is the size of the computational domain.

change L_b and observe in Fig. 7 that (here with $V=\beta=1$ $\gamma=1$, $\tau_s=0$) there is a critical size leading to the possibility of an initial growth of the bump. We notice that unfortunately, the bump does not move, the wind side part is longer and longer and the lee side has nearly a constant slope. Qualitatively same results are obtained for the subcritical and $A=0$ cases. Nearly the same results are obtained by Lagrée[22] with developing boundary layer so that the final position of the dune was fixed.

Second, for the sake of illustration of the ''stability'' of the supercritical case (with $V=\beta=1$, $\lambda=0$), an example of the wash out of a bump is presented in Fig. 8. Erosion takes place at the point where $\tau=0$, and the sediments are then convected. The bump is destroyed by the shear which is extreme just after the crest.

Third, we look at the lee side of the bump. Starting from a random noise distribution, first the wavelength $(2\pi/k_M)$ of maximal σ is selected (as already mentioned), after quite a long time a coarsening is observed (see next section). During a long time a configuration with three or four bumps may be observed. Here we observe the obtained bump shape after the crest in the lee side. Even if $\lambda=0$ a change of slope happens (see Figs. 7 and 9). This kink develops after the crest, it corresponds to the point where the RHS of Eq. (25) is zero.

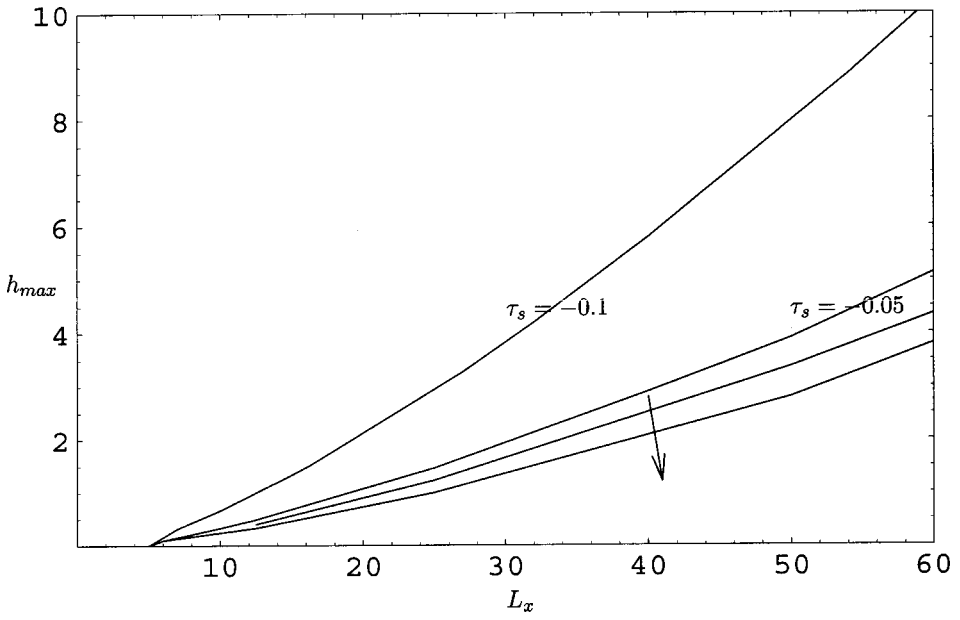

FIG. 11. The maximum of the final bump height $h_{\max}$ plotted as a function of half the domain size L_x in the case $A=0$. The case $\tau_s=-0.1$, $V=1$, $\lambda=0$ is the upper curve. The lower curves correspond to $\tau_s=-0.05$, $V=1$, the arrow is directed to the increasing values of λ ($\lambda=0$, 0.1, and 0.2). The subcritical case gives qualitatively the same results.

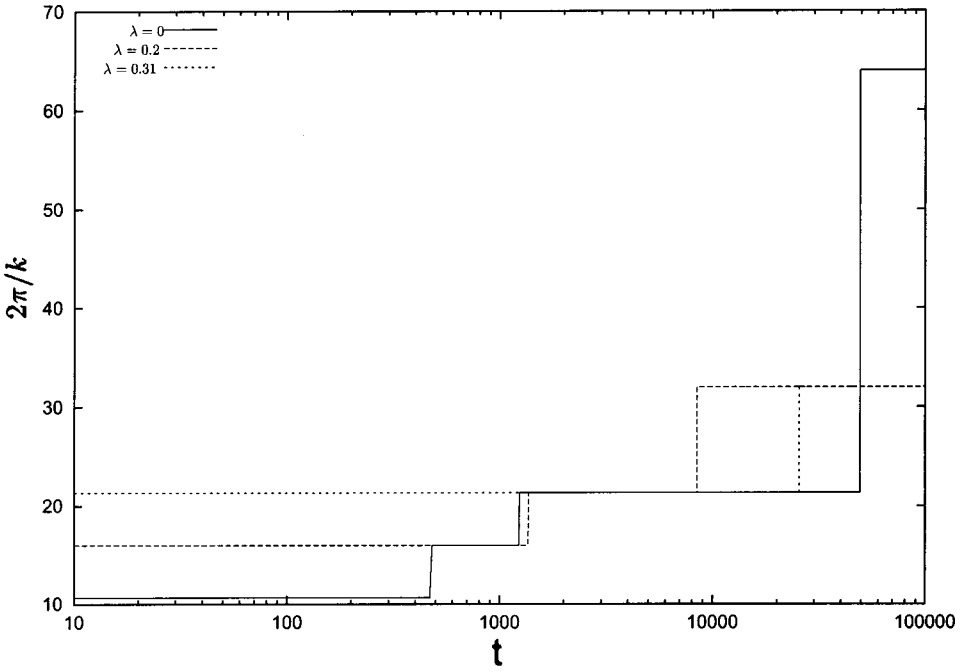

FIG. 12. Examples of long time evolution of $2\pi/k$ the wavelength value maximizing the bump spectrum (corresponding mostly to the number of bumps present in the domain). This is an infinite depth case for a domain of length $2L_x$. If $\lambda=0$, there is finally only one bump of size $2L_x$ (the largest possible). If $\lambda<0.316$, two bumps (of size L_x) are present, the larger are damped. If λ is increased, there is no dune anymore as predicted by the linearized theory of (28). Here $V=\beta=1$, $L_x=32$, $\tau_s=-0.25$. Notice that several bumps may live during a very long time: here in the case $\lambda=0.31$, during a very long time ($10<t<25\,000$) three bumps are present.

2. Long time evolution

Waiting much more longer (than in Fig. 5), we observe a kind of long wave slow instability: there are less and less bumps in the box (the small wave number gain an increasing importance). The mechanism is as follows: in the lee side of a bump, the skin friction is lesser than in the wind side (Fig. 2), so second bump in the lee-side of the first one experiences a smaller erosion than the first one.

The cases ($p=A$) and ($A=0$) evolve toward a one mode bump filling the domain (see Fig. 10 the $A=0$ case), the maximal height of the bump depends on the length of the computational domain. In Fig. 11 we plot the maximum of the bump as function of the size of the domain (in the case $A=0$, $\beta=\gamma=V=1$). Unsurprisingly, the larger $|\tau_s|$, the higher the bump; and the larger λ, the smaller the bump.

The Hilbert case results essentially in the same wavelength coarsening but it needs a far longer time to be observed. Several bumps stay during long intervals of time in the domain. In Fig. 12 we plot an example of such coarsening of the bump in the no slope effect case ($\lambda=0$). Notice that for $1500<t<50\,000$ three bumps are present in the box. The growth of the wavelength is more or less logarithmic. If now we introduce the slope effect in the equations in the Hilbert case, the result is, as predicted by Eq. (28) a damping of the unstable long waves (see Fig. 6), so that in the conditions chosen in Fig. 12 two bumps are ultimately present

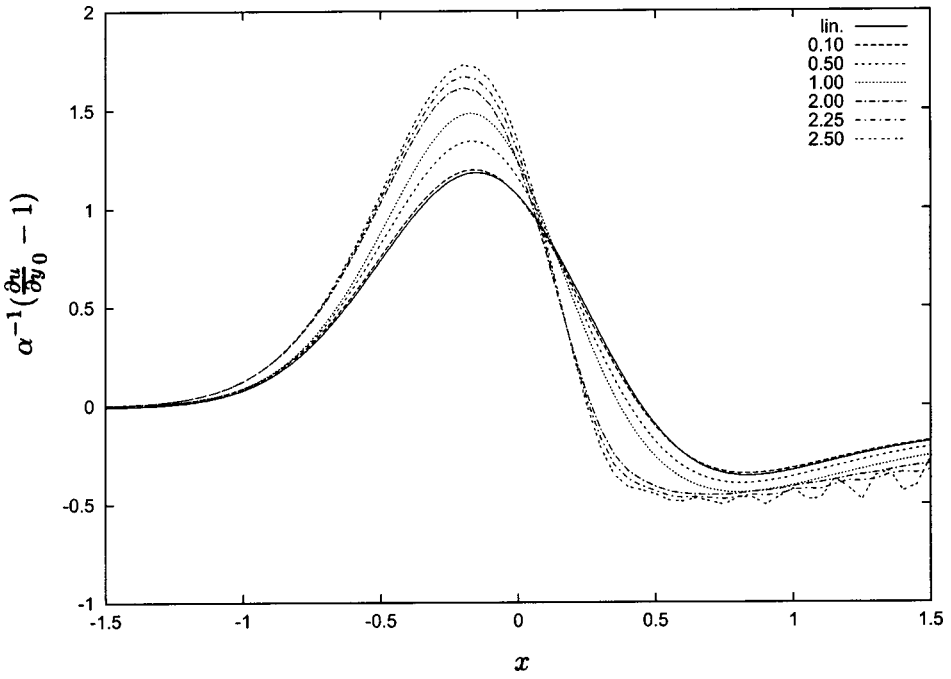

FIG. 13. The reduced wall shear $[(\partial u/\partial y_0)-1]/\alpha$ function of x, in the $A=0$ case, for the bump $\alpha e^{-\pi x^2}$ with $\alpha=0.10$, $\alpha=0.5$, $\alpha=1.0$, $\alpha=2$, $\alpha=2.25$, $\alpha=2.50$. The plain curve (''lin.'') is the linear prediction (14), other curves come from the nonlinear numerical solution. The nonlinearity increases the relative maximum value of the shear stress, but weakly shifts it downstream. There is also a decrease of the relative width of the curve. Notice the numerical oscillations in the case of separated flow (separation is for $\alpha>2.1$)

(cases $\lambda=0.2$ and $\lambda=0.316$). Enlarging gradually the domain up to twice allows another bump to be present. As predicted again by (28) [and (29)], when $V=1$, $\beta=1$, there is a limiting value $\lambda=0.316$, if λ is greater, then the flat bottom is stable (Fig. 12).

V. CONCLUSION

We have presented here a simplified model of flow over an erodible bed which is asymptotically coherent (in a 2D laminar linearized description at large Reynolds number). The advantage of this model is that a lot of hydrodynamical mechanisms have been put without usual integral simplifications, or without a complete Navier–Stokes numerical simulation. Though we do not claim that we have a ''real'' model, we have caught some features with a realistic asymptotic solution of the Navier–Stokes equations. Furthermore, the selected method allows to obtain some analytical results such as the growth rate (28).

To sum up, the equation of transport of sediments contains the following terms: a convective effect between q the flux of sediments and τ the perturbation of skin friction, a threshold effect for τ and a limiting slope effect (through the parameter λ). This effect of the convection of sediments has been justified on view of the equation of transported sediments, but may be seen as a simple balance law at the wall. The linear stability analysis gives good predictions for the numerical solution because the nonlinearity lies only in the threshold pick up relation. Various hydraulic regimes have been introduced in the selected framework. The supercritical case, in this description with convection, leads always to the destruction of the bump. Three other regimes (infinite depth, subcritical case, shear flow) result in temporal instability for any wave length k if no convective and slope effects are present. Introducing convective effect damps the large wave numbers (it helps for the numerical simulations); introducing slope effect damps the large wave numbers as well (Charru *et al.* results are recovered in their ''deep viscous regime'').

Furthermore in the sole infinite depth case, this slope effect damps small wave numbers as well: this promotes a ''ripple mode.'' Only a narrow band of frequencies is amplified, so that, instead of a continuous coarsing leading to one single bump in the domain, a final train of bump is obtained.

Of course, the first hypothese to be introduced in the model to be more realistic would consit in a turbulent stress viscosity and diffusivity. Before this, other hypothesis may be removed one after the other. For example, a slope limitation model could easily be introduced instead of the diffusive effect of $\lambda\ldots$, a full nonlinear resolution for the fluid would illuminate the real effect of flow separation. This will result in an increasing complexity of the final numerical solution.

ACKNOWLEDGMENT

This work was supported by ACI ''Jeunes Chercheurs'' No. 2314.

APPENDIX: NONLINEAR FLOW SEPARATION

In this appendix we compare, for a given bump, the linearized solution of (9)–(12) in the zero displacement case (8):

$$FT[\tau]=\frac{(-ik)^{2/3}}{\mathrm{Ai}'(0)}\mathrm{Ai}(0)\frac{FT[f]}{\beta^*-\beta_{pf}},$$

with $\beta^*=(3\,\mathrm{Ai}'(0))^{-1}(-ik)^{1/3}$ and (8): $\beta_{pf}=0$, and a complete non linear solution of (9)–(12) with (8). We compute the skin friction for various values of the high α of a bump $y_w=\alpha\exp(-\pi x^2)$. We observe that the separation for this kind of bump occurs for $\alpha\simeq 2.1$. The computations are possible when the skin friction is smaller than zero (the triple deck is the asymptotic framework for separated flows, there is no Goldstein singularity), but if the size of the separation bubble is too big, numerical oscillations take place ($\alpha\simeq 2.5$). In Fig. 13 we plot the reduced skin friction $\alpha^{-1}[(\partial u/\partial y)\,|_0-1]$, because the linear prediction of (14) is

$$\left.\frac{\partial u}{\partial y}\right|_0=1+\alpha FT^{-1}[(3\,\mathrm{Ai}(0))(-ik)^{1/3}FT[f]]+O(\alpha^2). \tag{A1}$$

We see that for $\alpha=0.1$ the agreement between the linear and nonlinear solution is excellent. Larger values of α induce the discrepancy observed on the Fig. 13 which is an increase of the maximum of the skin friction value and a decrease of its relative width.

[1] C.T. Yang, *Sediment Transport: Theory and Practice* (McGraw-Hill, New York, 1995), p. 480.
[2] J. Fredsøe and R. Deigaard, ''Mechanical of coastal sediment transport,'' *Advanced Series on Ocean Engineering* (World Scientific, Singapore, 1992), Vol. 3.
[3] P. Nielsen, ''Coastal bottom boundary layers and sediment transport,'' *Advanced Series on Ocean Engineering* (World Scientific, Singapore, 1992), Vol. 4.
[4] K. Kroy, G. Sauerman, and H.J. Herrmann, ''A minimal model for sand dunes,'' ArXiv: cond-mat/0101380.
[5] G. Sauermann, K. Kroy, and H.J. Herrmann, ''Continuum saltation model for sand dunes,'' Phys. Rev. E **64**, 031305 (2001).
[6] K.H. Andersen, ''A particle model of rolling grain ripples under waves,'' Phys. Fluids **13**, 58 (2001).
[7] H. Nishimori, M. Yamasaki, and K.H. Andersen, ''A simple model for the various pattern dynamics of dunes,'' Int. J. Mod. Phys. B **12**, 257 (1998).
[8] K.H. Andersen, M.-L. Chabanol, and M.v. Hecke, ''Dynamical models for sand ripples beneath surface waves,'' Phys. Rev. E **63**, 066308 (2001).
[9] K.H. Andersen and J. Fredsøe, ''How to calculate the geometry of vortex ripples,'' Proceedings of the conference ''Coastal Sediments,'' Long Island, 1999.
[10] P.S. Jackson and J.C.R. Hunt, ''Turbulent wind flow over a low hill,'' Q. J. R. Meteorol. Soc. **101**, 929 (1975).
[11] J.E. Plapp and J.P. Mitchell, ''A hydrodynamic theory of turbidity current,'' J. Geophys. Res. **65**, 983 (1960).
[12] J. Akiyama and H. Stefan, ''Turbidity current with erosion and deposition,'' J. Hydraul. Eng. **111**, 1473 (1985).
[13] J. Zeng and D.R. Lowe, ''Numerical simulation of turbidity current flow and sedimentation,'' Sedimentology **44**, 67 (1997).
[14] V.Ya. Neiland, ''Propagation of perturbation upstream with interaction between a hypersonic flow and a boundary layer,'' Mekh. Zhidk. Gaza **4**, 53 (1969).
[15] F.T. Smith, ''On the high Reynolds number theory of laminar flows,'' IMA J. Appl. Math. **28**, 207 (1982).
[16] V.V. Sychev, A.I. Ruban, V.V. Sychev, and G.L. Korolev, *Asymptotic Theory of Separated Flows* (Cambridge University Press, Cambridge, 1998).
[17] F.T. Smith, ''On physical mechanisms in 2 and 3 dimensional separation,''

Philos. Trans. R. Soc. London, Ser. A **358**, 3091 (2000).
[18]S. Bhattacharyya, S.R.C. Dennis, and F.T. Smith, ''Separating flow past a surface-mounted blunt obstacle,'' J. Eng. Math. **3**, 47 (2001).
[19]F. Charru and H. Mouilleron-Arnould, ''Instability of a bed of particules sheared by a viscous flow,'' J. Fluid Mech. **452**, 303 (2002).
[20]A.C. Fowler, ''Dunes and drumlins,'' in *Geomorphological Fluid Mechanics*, edited by N.J. Balmforth and A. Provenzale, Lecture Notes in Physics 582 (Springer, New York, 2001), pp. 430–454.
[21]U. Schlafinger, A. Acrivos, and K. Zhang, ''Viscous resuspension of a sediment within a stratified flow,'' Int. J. Multiphase Flow **16**, 567 (1990).
[22]P.-Y. Lagrée, ''Erosion and sedimentation of a bump in fluvial flow,'' C. R. Acad. Sci., Ser. IIb: Mec., Phys., Chim., Astron. **328**, 869 (2000).
[23]H. Schlichting, *Boundary Layer Theory*, 7th ed. (McGraw Hill, New York, 1987).
[24]F.J. Higuera, ''The hydraulic jump in a viscous laminar flow,'' J. Fluid Mech. **274**, 69 (1994).
[25]F.J. Higuera, ''Opposing mixed convection flow in a wall jet over a horizontal plate,'' J. Fluid Mech. **342**, 355 (1997).
[26]P.-Y. Lagrée, ''Removing the marching breakdown of the boundary-layer equations for mixed convection above a horizontal plate,'' Int. J. Heat Mass Transfer **44**, 3359 (2001).
[27]M. Van Dyke, *Perturbation Methods in Fluid Mechanics* (Parabolic, Stanford, CA, 1975).
[28]K. Stewartson and P.G. Williams, ''Self-induced separation,'' Proc. R. Soc. London, Ser. A **312**, 181 (1969).
[29]J. Gajjar and F.T. Smith, ''On hypersonic self induced separation, hydraulic jumps and boundary layer with algebraic growth,'' Mathematika **30**, 77 (1983).
[30]R.L. Bowles and F.T. Smith, ''The standing jump: theory, computations and comparisons with experiments,'' J. Fluid Mech. **242**, 145 (1992).
[31]P.G. Baines, *Topographic Effects in Stratified Flows* (Cambridge University Press, Cambridge, 1995).
[32]A. Kluwick, A. Exner, and E.A. Cox, ''Structure of small amplitude hydraulic jumps in laminar high Reynolds number flow,'' 4th Euromech Fluid Mechanics Conference, Eindhoven, 19–23 November 2000, p. 61.
[33]L. Plantier, ''Le problème de la couche interne des écoulements asymptotiques de type triple couche: modèle, analyse et simulations,'' thèse Université Paul-Sabatier, Toulouse, France, 1997.
[34]F.T. Smith, ''Flow through constricted or dilated pipes and channels,'' Q. J. Mech. Appl. Math. **29**, 343 (1976).
[35]F.T. Smith, P.W.M. Brighton, P.S. Jackson, and J.C.R. Hunt, ''On boundary layer flows past two dimensional obstacles,'' J. Fluid Mech. **113**, 123 (1981).
[36]B. Andreotti, P. Claudin, and S. Douady, ''Selection of dune shapes and velocities. Part 2: A two-dimensional modelling,'' Eur. Phys. J. B **28**, 341 (2002).
[37]Y. Noh and H.J.S. Fernando, ''Dispersion of suspended particules in turbulent flow,'' Phys. Fluids A **3**, 1730 (1991).
[38]G. Seminara, ''Invitation to sediment transport,'' in *Geomorphological Fluid Mechanics*, edited by N. J. Balmforth and A. Provenzale, Lecture Notes in Physics 582 (Springer, New York, 2001), pp. 394–402.
[39]N. Izumi and G. Parker, ''Inception of channelization and drainage basin formation: upstream-driven theory,'' J. Fluid Mech. **283**, 341 (1995).
[40]N.L. Komarova and S.M.H. Hulscher, ''Linear inst. mechanisms for sand wave formation,'' J. Fluid Mech. **413**, 219 (2000).
[41]J.-P. Bouchaud, M.E. Cates, J. Ravi Prakash, and S.F. Edwards, ''A model for the dynamics of sand pile surfaces,'' J. Phys. I **4**, 1383 (1994).
[42]A. Valance and F. Rioual, ''A nonlinear model for aeolian sand ripples,'' Eur. Phys. J. B **10**, 5543 (1999).
[43]T. Boutreux, E. Raphael, and P.G. de Gennes, ''Surface flows of granular materials: A modified picture for thick avalanche,'' Phys. Rev. E **58**, 4692 (1998).
[44]J.F. Kennedy, ''The mechanics of dunes and antidunes in erodible-bed channels,'' J. Fluid Mech. **16**, 521 (1963).
[45]F. Engelund and J. Fredsøe, ''Sediment ripples and dunes,'' Annu. Rev. Fluid Mech. **14**, 13 (1982).
[46]P. Blondeaux, ''Sand ripples under sea waves,'' J. Fluid Mech. **90**, 1 (1990).
[47]K.J. Richards, ''The formation of ripples and dunes on an erodible bed,'' J. Fluid Mech. **99**, 597 (1980).